



Equalization method for Medipix3RX



Jean Rinkel^{a,*}, Debora Magalhães^a, Franz Wagner^a, Erik Frojdh^b, Rafael Ballabriga Sune^b

^a Brazilian Synchrotron Light Laboratory (LNLS/CNPEM), Rua Giuseppe Máximo Scolfaro, 10.000, Caixa Postal 6192, 13083-970 Campinas, SP, Brazil

^b CERN, Route de Meyrin 385, Geneva, Switzerland

ARTICLE INFO

Article history:

Received 14 April 2015

Received in revised form

12 August 2015

Accepted 13 August 2015

Available online 21 August 2015

Keywords:

Hybrid semiconductor detector

Medipix3RX

Threshold equalization

Energy resolution

ABSTRACT

This paper describes a new method of threshold equalization for X-ray detectors based on the Medipix3RX ASIC, using electrical pulses to calibrate and correct for the threshold dispersion between pixels. This method involves a coarse threshold tuning, based on two 8 bits global DACs and which sets the range of variation of the threshold values; and a fine-tuning, based on two 5-bits adjustment DACs per pixel. As our fine-tuning approach is based on a state-of-the-art methodology, our coarse tuning relies on an original theoretical model. This model takes into account the noise level of the ASIC, which varies with temperature and received radiation dose. The experimental results using 300 μm Si sensor and $K\alpha$ fluorescence of Zn show a global energy resolution improvement of 14% compared to previous equalization methods. We compared these results with the best achievable global energy resolution given by the resolution of individual pixels and concluded that the remaining 14% difference was due to the discretization error limited by the number of equalization bits.

© 2015 CERN for the benefit of the Authors. Published by Elsevier B.V. This is an open access article under the CC BY license (<http://creativecommons.org/licenses/by/4.0/>).

1. Introduction

Hybrid silicon photon-counting detectors can meet the requirements of very high dynamic range and high detection efficiency, especially needed for tomographic applications using synchrotron radiation. Compared to other families of hybrid pixel detectors, such as Pilatus [1] and XPAD [2], the Medipix3RX readout chip enables a higher spatial resolution, with a pixel size of 55 μm by 55 μm . Furthermore, this chip takes advantage of the 130 nm CMOS technology to allow a high level of functionality in each pixel, enabling correction of the charge diffusion in the sensor (charge summing mode) or allowing up to 8 energy thresholds per cluster of four pixels (spectroscopic mode).

Equalization procedures are fundamental steps to limit the dispersion between pixels, in terms of relationship between threshold and energy for hybrid counting detectors. Dispersion in the electrical parameters between pixels is intrinsic to the nature of the CMOS transistors used for the pixel circuit implementations. The previous generation of the Medipix ASIC, the Medipix2, has an architecture based on a 3-bit fine adjustment for each pixel, which lead to various equalization approaches based on electrical pulses, electronic pixel noise, monochromatic X-ray or γ source [3] and even polychromatic sources [4].

Medipix3RX offers the possibility to perform the equalization using

- Two 5-bits adjustment DACs (Digital-to-Analog Converter) per pixel, denoted by DAC_ConfigDiscl[0:4] and DAC_ConfigDisch [0:4] to adjust the thresholds THL (Threshold Low) and THH (Threshold High), respectively. These thresholds are related to the two 12 bits counters per pixel, COUNTERL and COUNTERH.
- Two 8-bits global DACs which set the range of variation of the thresholds THL and THH values within the 5 bits, denoted by DAC_Discl and DAC_Disch.

Fig. 1 shows the block diagram of the pixel circuitry. THL and THH are denoted by TH[0] and TH[1] respectively.

This equalization requires measurements to estimate the threshold dispersion using the electronic noise level, X-ray acquisitions or injection of pulses on the chip to simulate the current generated by real photons (test pulse mode). In this paper, we will focus on the equalization of the first counter (THL) by proposing a method to optimize DAC_Discl, which refers to the DAC in the periphery setting the least significant bit current (I_{LSB}), and DAC_ConfigDiscl, which refers to the 5 bits per pixel configuration without loss of generality. We adopted first the test pulse mode for the measurements to compare the proposed equalization procedure with other methods. Then, the performances of the different algorithms were compared using monochromatic X-ray radiation obtained from the $K\alpha_1$ and $K\alpha_2$ characteristic X-ray lines of Zn.

* Corresponding author. Tel.: +55 19 3518 3192; fax: +55 19 3512 1004.

E-mail address: jean.rinkel@lnls.br (J. Rinkel).

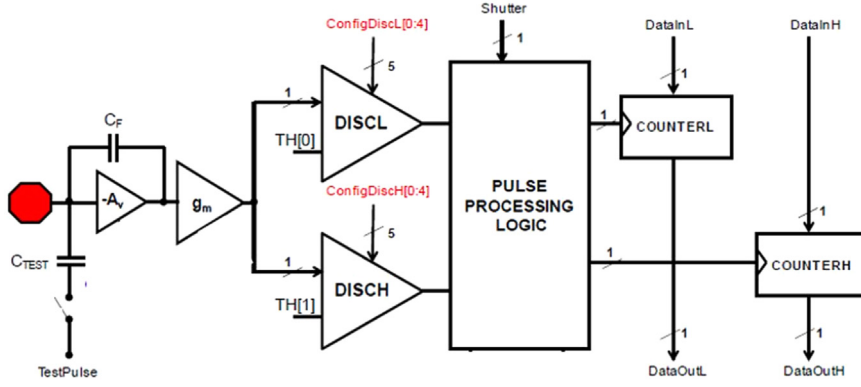


Fig. 1. Block diagram of the pixel circuitry when programmed in Fine Pitch Mode with Single Pixel Mode of operation.

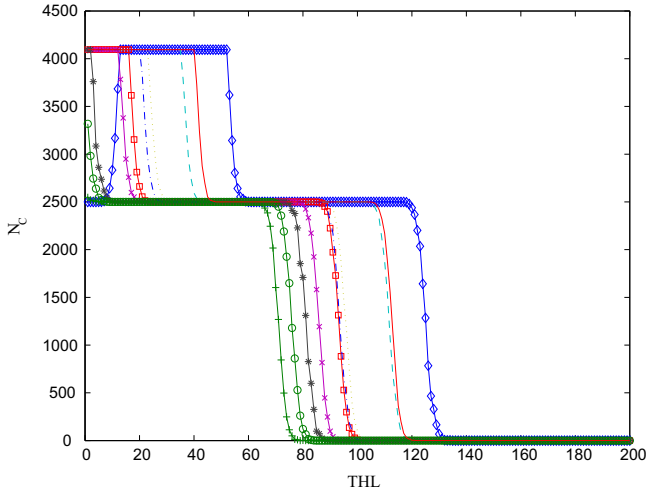


Fig. 2. THL scan in test pulse mode for 10 different pixels before equalization (DAC_DiscL=50 - DAC_ConfigDiscL=15, Number of pulses $N_{pulses}=2500$).

2. Material and method

2.1. Detector

Measurements were performed with a Medipix3RX ASIC bump-bonded to a 300 μm silicon sensor. The chip was used in conventional single-pixel mode configured with 12-bit counters and super high-gain mode [5]. The detector was read out using Fitpix USB interface for Medipix3RX and Pixelman software, both developed by the Institute of Experimental and Applied Physics (IEAP) [6].

2.2. Threshold evaluation method

Medipix3RX can operate in electrical calibration mode: a calibration charge can be injected in each analog chain of the ASIC using a test capacitor. To generate the constant input signal, a voltage step pulse with a programmed amplitude is injected through the injection test capacitor present on each pixel. Each pixel is pulsed a user-defined number of times during the shutter opening interval and the ratio of recorded hits divided by the number of input pulses is registered and plotted against the value of THL. The result of this scan is a s-shaped curve for each pixel.

The run is made of this basic scan of threshold reference voltage for the amplitude corresponding to the equalization energy. For a given calibration-pulse height, the number of output counts (N_c) depends on the effective threshold voltage and on the number of calibration pulses sent. An example of 10 threshold

scans of individual pixels is shown in Fig. 2, for a pulse amplitude corresponding to a 8 keV X-ray photon. When the threshold is set at the noise floor, the counter associated to THL (24 bits) overflows.

We followed a state-of-the-art method [7] to evaluate the threshold value in each pixel corresponding to a given electric pulse height. This threshold voltage is referred to as th^* . As the function $N_c(THL) - N_{pulses}/2$ is an antisymmetric function around th^* , the zero-crossing could be used to find th^* . However, as shown in Ref. [7], correlating $N_c(THL) - N_{pulses}/2$ with an appropriately chosen symmetric function f_{sym} keeps the same zero-crossing value but improves the precision and repeatability of the measurement. The result of the correlation is denoted by f_{corr}

$$f_{corr}(th) = \int \left(N_c(THL) - \frac{N_{pulses}}{2} \right) f_{sym}(THL - th) dTHL \quad (1)$$

The symmetric function is defined by the following equations:

$$f_{sym}(th) = \begin{cases} 0 & \text{if } th < -m \sigma \text{ or if } th > m \sigma \\ \frac{th + m \sigma}{m \sigma} & \text{if } -m \sigma \leq th < 0 \\ -\frac{th + m \sigma}{m \sigma} & \text{if } 0 \leq th \leq m \sigma \end{cases} \quad (2)$$

with $m=2.5$ being an empirical parameter and σ is the energy resolution of each individual pixel, being 0.85 keV the typical energy resolution (R.M.S.) of the analog chains.

2.3. Threshold fine tuning

Fine tuning is performed by adjusting the individual 5-bits DACs for each pixel (DAC_ConfigDiscL). First, a pixel-per-pixel calibration of the linear relationship between th^* and DAC_ConfigDiscL is done by finding th^* values for at least two different DAC_ConfigDiscL values, denoted D_1 and D_2 (for example 0 and 31). For the pixel indexed by i , the corresponding th^* values are denoted $th_1^*(i)$ and $th_2^*(i)$. We perform then a threshold scan with a target value of DAC_ConfigDiscL, denoted D_{target} (for example 15). The mean value of th^* over the pixels is denoted th_{target}^* . For the pixel indexed by i , the adjusted DAC_ConfigDiscL value is given by

$$\text{DAC_ConfigDiscL}(i) = \frac{D_2 - D_1}{th_2^*(i) - th_1^*(i)} \times (th_{target}^* - th_2^*(i)) + D_2 \quad (3)$$

2.4. Threshold coarse tuning – global range optimization

After equalization, the threshold position of the pixel indexed by i is denoted by $th_{eq}(i)$. The figure of merit chosen to evaluate the

equalization is the root mean square error ϵ defined as:

$$\epsilon = \sqrt{\frac{1}{N_{\text{pixels}}} \sum_i \left(th_{eq}(i) - \frac{1}{N_{\text{pixels}}} \sum_i th_{eq}(i) \right)^2} \quad (4)$$

where N_{pixels} refers to the number of pixels of the chip. ϵ is expressed in units of threshold level.

It is demonstrated in [Annex 1](#) that minimizing the root mean square error is equivalent to minimize the global energy resolution expressed in terms of Full Width at Half Maximum (FWHM) of a monochromatic energy peak. The global energy resolution of the detector is made of two contributions: electronic noise per pixel and threshold dispersion. The threshold dispersion has two sources: variation in zero level, and variation in gain. When equalizing with the noise, the threshold dispersion is minimized at an equivalent energy of 0 keV. The more we increase the energy in the measurement, the more the dispersion between pixels increases due to gain mismatch. When equalizing with test pulses or with real photons, we minimize the effect of the gain variation at the energy we set the test pulses or the incoming beam. The root mean square error can be expressed as a function of different parameters. First, the gain of DAC_ConfigDiscl, denoted by Δ , is defined as the range of threshold variation for each pixel between the two extreme values of the 5 bits adjustment DACs per pixel (DAC_ConfigDiscl=0 and $2^5 - 1 = 31$). This last parameter varies between pixels. The standard deviation of the threshold between pixels for the same DAC_ConfigDiscl value is denoted by σ , which corresponds to the non-equalized threshold dispersion. [Fig. 3](#) shows measured histograms of the th^* thresholds for 3 different DAC_DiscL values. We draw the mean value of Δ and σ .

We developed a theoretical model for the root mean square error

$$\epsilon^2 = \epsilon_d^2 \operatorname{erf}\left(\frac{\Delta}{2\sqrt{2}\sigma}\right) + \frac{\Delta^2}{4} \left(1 - \operatorname{erf}\left(\frac{\Delta}{2\sqrt{2}\sigma}\right)\right) - \frac{2}{\sqrt{2\pi}} \sigma \Delta \exp\left(\frac{-\Delta^2}{8\sigma^2}\right) + 2 \int_{\Delta/2}^{\infty} \frac{x^2}{\sqrt{2\pi}} e^{-\frac{x^2}{2\sigma^2}} dx \quad (5)$$

In this equation, ϵ_d , in units of *THL*, represents the root mean square error due to discretization and to the th_{eq} reproducibility. The th_{eq} reproducibility is characterized by the standard deviation of the threshold position th_{eq} for the same pixel and DAC values. This standard deviation of the random noise of individual pixel for a given range Δ_0 (fixed by the value of DAC_DiscL) is denoted by σ_{RO} . This quantity depends on the noise level of the ASIC, which

varies with temperature and received radiation dose. ϵ_d is given by

$$\epsilon_d^2 = \frac{1}{\delta} \int_{-\infty}^{+\infty} \frac{x^2}{2} \left[\operatorname{erf}\left(\frac{\delta/2-x}{\sqrt{2}\sigma_{RO} \frac{\Delta}{\Delta_0}}\right) + \operatorname{erf}\left(\frac{\delta/2+x}{\sqrt{2}\sigma_{RO} \frac{\Delta}{\Delta_0}}\right) \right] dx \quad (6)$$

where δ is the threshold step and is defined by

$$\delta = \frac{\Delta}{2^5 - 1} \quad (7)$$

For a perfect reproducibility, a straightforward calculation gives us: $\epsilon_d^2 = \delta^2/12$. This is the maximum achievable precision, which corresponds to the discretization error. Eqs. (5) and (6) are detailed in the [Annex 2](#).

2.5. Algorithm

The overall procedure can be divided into five different steps:

1. Perform scans for different values of DAC_DiscL and DAC_ConfigDiscl. From these scans, we deduce the values of σ and Δ corresponding to each DAC_DiscL.
2. Run the fine tuning routine described in [Section 2.3](#) for some DAC_DiscL values, and use the results and Eq. (5) to find σ_{RO} .
3. Find the optimal value of Δ based on Eq. (5) and the measured values of σ and σ_{RO} .
4. Use the results from step (1) and the optimal Δ value to find the optimal DAC_DiscL value.
5. Re-run the fine tuning procedure with the optimal DAC_DiscL value.

3. Results

3.1. Threshold coarse tuning

[Fig. 4](#) shows the relationship between DAC_DiscL and the ratio of the range Δ divided by σ . To compare experimental data with the model of Eq. (5), a fitting procedure based on least square difference criterion was applied to the experimental values of ϵ^2 to find the σ_{RO} parameter. The optimized value of σ_{RO} was 0.61, in units of *THL*. Theoretical curves are plotted in [Fig. 5](#) using the estimated experimental noise, without noise and with the noise corresponding to the fitted value multiplied by factors of 2 and 3. The results show that the root mean square error clearly increases

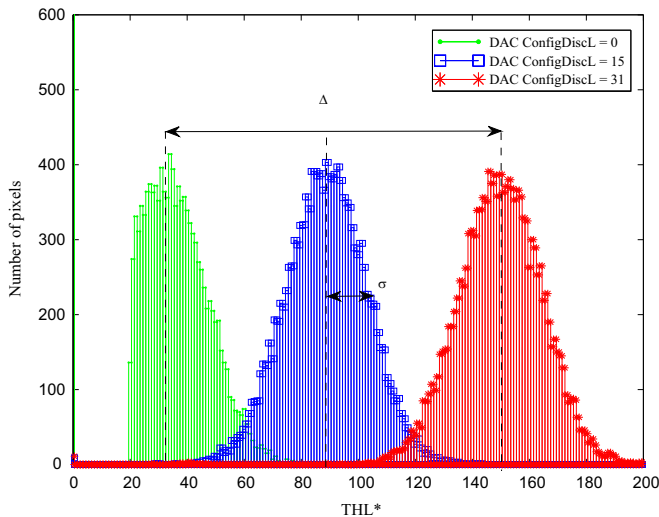


Fig. 3. Measured histograms of the thresholds for DAC_ConfigDiscl=0, 15 and 31 (DAC_DiscL=50).

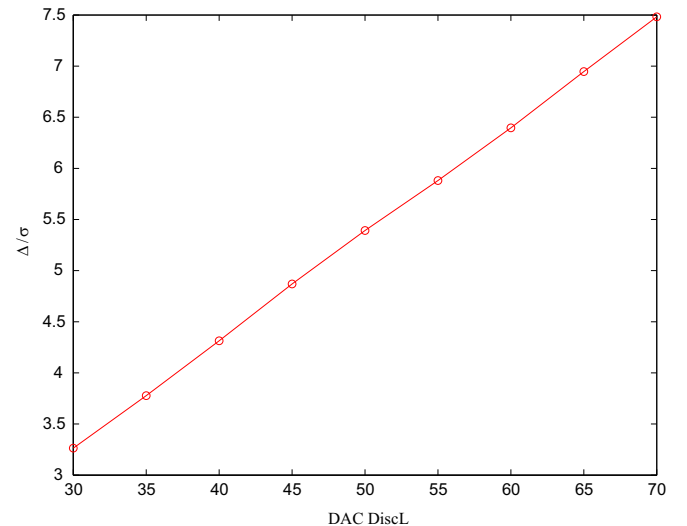


Fig. 4. Measured relationship between DAC_DiscL and the ratio of the range divided by σ .

with noise. The existence of optimal values of Δ/σ in the curves of Fig. 5 comes from the trade-off between increasing discretization errors for high values of Δ/σ and increasing numbers of pixels out of the range of equalization for low Δ/σ values. Since the error of discretization includes σ_{R0} , characterizing the effect of noise level, the weight of this error increases with noise level. As a result, the values of Δ/σ minimizing the root mean square error tend to decrease with increasing noise, as showed in Table 1.

3.2. Energy resolution using test pulse and fluorescent target

After equalization, we scanned the THL threshold using the same test pulse parameters as the ones used for equalization to estimate the energy resolution. This energy resolution is defined as the Full Width at Half Maximum (FWHM) of the sum of the different differential scans of different pixels. Fig. 6 shows the spectra obtained with two reference equalization methods and with the new method. The state-of-the-art equalization procedure relies on noise floor [8] and is referred to as “noise”. The same algorithm was applied using test pulses instead of noise floor (reference). The main parameters for the three methods are

- Noise, DAC DiscL=73 ($\Delta/\sigma=7.3$).
- Test pulse (reference), DAC DiscL=81 ($\Delta/\sigma=8.1$).
- Test pulse (new), DAC DiscL=53 ($\Delta/\sigma=5.7$).

To validate the new method with real photons, we did a THL scan of a fluorescence spectrum obtained by irradiating a Zn target with an X-ray generator at 45°. We measured simultaneously $K\alpha_1$ and $K\alpha_2$ (8.639 and 8.616 keV respectively). In order to attenuate $K\beta_1$ and $K\beta_2$ (9.572 and 9.572 keV respectively), we used a copper filter placed in front of the detector (K edge of 8.993 keV). Fig. 7 shows the spectra obtained with the three equalization methods.

Table 2 shows the global energy resolution of a single chip Medipix3RX assembly obtained with the reference equalization

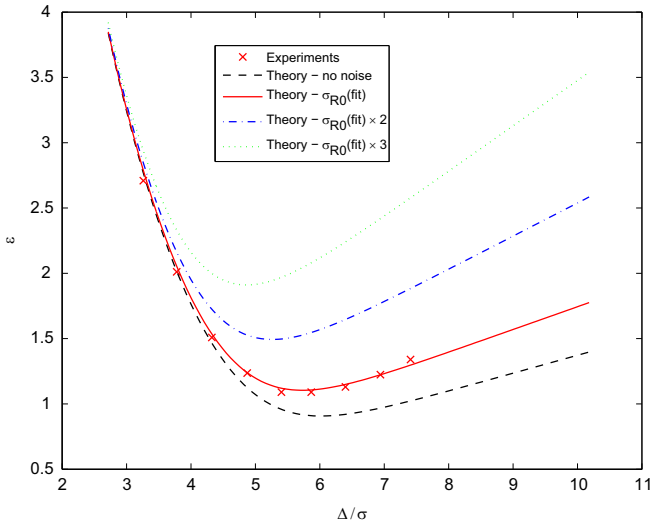


Fig. 5. Experimental mean error vs. theoretical values for different noise levels, with σ_{R0} (fit)=0.61.

Table 1
Evaluation of the optimal configuration for different noise levels

Simulated noise	No noise	σ_{R0}	$\sigma_{R0} \times 2$	$\sigma_{R0} \times 3$	$\sigma_{R0} \times 4$
Optimal Δ/σ	6.04	5.70	5.29	4.89	4.55

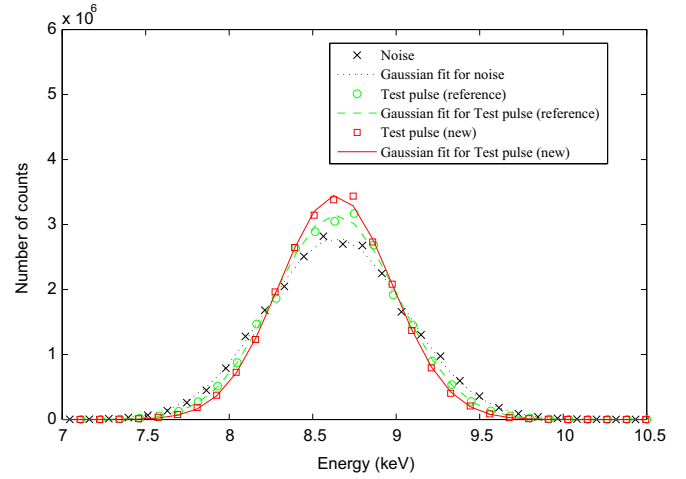


Fig. 6. Spectra obtained with the three equalization methods using a test pulse corresponding to 8.639 keV photons.

methods (using the electronic noise and the test pulse mode [8]) and with our original method of equalization. The resolution of individual pixels is the theoretically best achievable energy resolution (perfect equalization). These results show a significant improvement compared to the previous methods. We obtained a resolution of 0.79 keV and 1.08 keV at 8.639 keV using test pulse and Zn fluorescence, respectively. Compared with the noise equalization, we improved the resolution by 24% and 20% using test pulse and Zn fluorescence respectively. Compared with the test pulse equalization of reference, we improved the resolution by 10% and 14% using test pulse and Zn fluorescence respectively. The best achievable resolution defined by the resolution of individual pixels remains 14% lower than the resolution using the proposed method. The resolution of individual pixels was not calculated with Zn fluorescence since the photonic noise remains very high for acquisitions with limited statistics.

4. Discussion

The best achievable energy resolution was quantified using test pulse. Actually, if we do a threshold scan in a single pixel, the energy resolution is determined exclusively by the noise of the system and provides an indirect calculation of the noise of a single channel of the ASIC. The noise of the single analog chain was measured to 690 eV (FWHM) which is equivalent to 293 rms (standard deviation). The noise of a single channel can be deduced by dividing this last number by the average ionization energy of Si (3.62 eV for Si). Finally, we get a Medipix3RX single-channel noise in single pixel mode of 81 e⁻.

The method still needs to be optimized with respect to the duration of equalization. The dependence of the method with the electronic noise shows that, ideally, the equalization should be performed periodically, therefore requiring a faster method, only to correct this effect. Another aspect that will be studied is the robustness of equalization with the variation of energy, for example for applications requiring quick measurements at various energies. Finally, the proposed method could be adapted to perform the equalization with a monochromatic source (synchrotron radiation, fluorescence emission or gamma rays).

5. Conclusion

We developed a new method of threshold equalization for Medipix3RX ASIC. This method is based on a theoretical model for

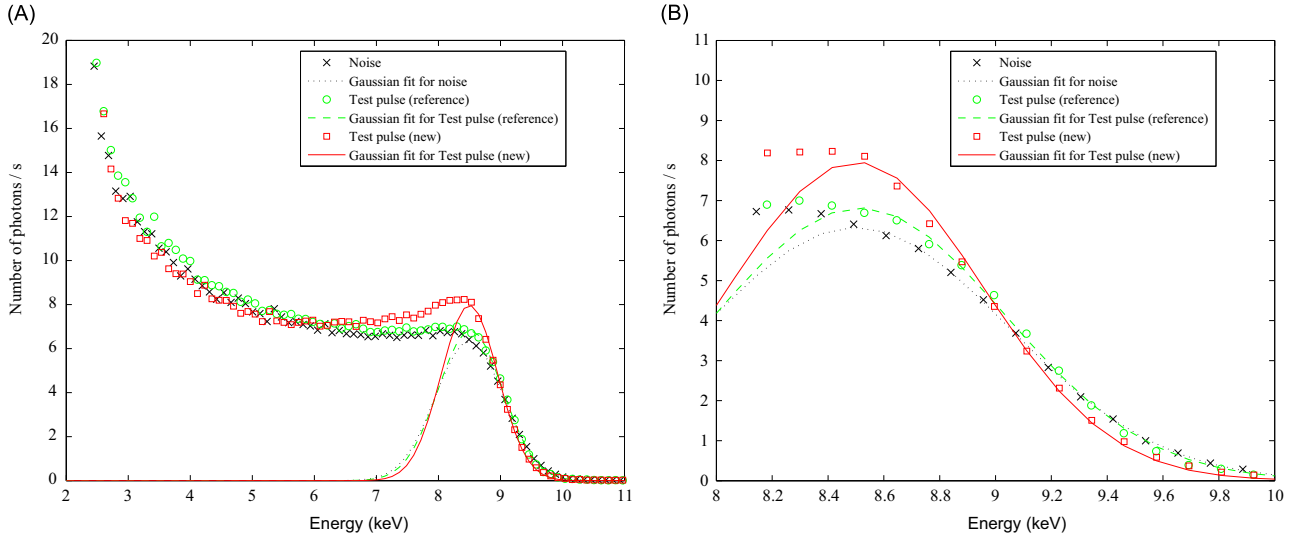


Fig. 7. Spectra obtained with the three equalization methods using Zinc K α fluorescence (8.639 and 8.616 keV photons): scan with charge-sharing plateau (A) and zoom on the fluorescence peak (B).

Table 2
Energy resolution (FWHM in keV at 8.639 keV) obtained with different equalization methods and theoretically best achievable energy resolution (individual pixels)

Equalization method	Noise	Test pulse (reference)	Test pulse (new)	Individual pixels
Test pulse	0.98	0.87	0.79	0.69
Zn fluorescence	1.2864	1.2260	1.0759	

coarse tuning. This model enables to adapt the equalization to the detector noise level. The results of the equalization show a global energy resolution improvement of 14% compared to previous methods (1.08 keV vs. 1.23 keV at 8.639 keV with Zn fluorescence X-ray photons). We concluded that the 14% difference with the best achievable energy resolution (0.79 keV vs. 0.69 keV with test pulse measurements) was due to the discretization error limited by the number of equalization bits.

6. Annex

6.1. Annex 1

The purpose of this paragraph is to express the global energy resolution of the detector as a function of the dispersion between thresholds of individual pixels. Here, we consider that the chip is equalized at the energy of the monochromatic irradiation. The differential scan of the threshold th of each pixel, indexed by i , is a distribution, denoted by $f_i(th)$, with mean value $th_{eq}(i)$. Let us denote σ_i the standard deviation of this distribution. The global threshold distribution F is

$$F(th) = \frac{1}{N_{pixels}} \sum_{i=1}^{N_{pixels}} f_i(th) \quad (8)$$

The variance of the F distribution can be calculated by

$$\sigma_F^2 = \frac{1}{N_{pixels}} \int_{-\infty}^{+\infty} \sum_{i=1}^{N_{pixels}} f_i(th) (th - th_{mean})^2 dth \quad (9)$$

With

$$th_{mean} = \frac{1}{N_{pixels}} \int_{-\infty}^{+\infty} \sum_{i=1}^{N_{pixels}} f_i(th) dth = \frac{1}{N_{pixels}} \sum_{i=1}^{N_{pixels}} th_{eq}(i) \quad (10)$$

Developing (8) and (9) we get

$$\sigma_F^2 = \frac{1}{N_{pixels}} \sum_{i=1}^{N_{pixels}} \sigma_i^2 + \epsilon^2 \quad (11)$$

where ϵ^2 is the root mean square error defined by

$$\epsilon^2 = \frac{1}{N_{pixels}} \sum_i \left(th_{eq}(i) - \frac{1}{N_{pixels}} \sum_i th_{eq}(i) \right)^2 \quad (12)$$

The first term of Eq. (11) is the mean value of the variance of individual pixels. Finally, we demonstrated that optimizing the standard deviation of the global distribution is equivalent to optimize the root mean square error of the threshold positions of the pixels.

6.2. Annex 2

Let's consider that the threshold distribution for a constant mean DAC_ConfigDiscl value (=15) has a Gaussian distribution. The standard deviation and mean value are represented by σ and th_0 respectively. $err(th^* - th_0)$ refers to the RMS error after equalization for a threshold position equal to th^* before equalization and measured with DAC_ConfigDiscl=15. The root mean square error after equalization is

$$\begin{aligned} \epsilon^2 &= \int_{-\infty}^{+\infty} err(th^* - th_0)^2 \frac{1}{\sqrt{2\pi}\sigma} e^{-\frac{(th^* - th_0)^2}{2\sigma^2}} dth^* \\ &= \int_{-\infty}^{+\infty} err(th^*)^2 \frac{1}{\sqrt{2\pi}\sigma} e^{-\frac{th^{*2}}{2\sigma^2}} dth^* \end{aligned} \quad (13)$$

We can calculate ϵ^2 by summing two terms: ϵ_{in} is the root mean square error for the pixels within the equalization range $[-\Delta/2, \Delta/2]$ and ϵ_{out} is the root mean square error for the pixels out of it. Then we have

$$\epsilon^2 = \epsilon_{in}^2 + \epsilon_{out}^2 \quad (14)$$

With

$$\epsilon_{in}^2 = \int_{-\Delta/2}^{\Delta/2} err(th^*)^2 \frac{1}{\sqrt{2\pi}\sigma} e^{-\frac{th^{*2}}{2\sigma^2}} dth^* \quad (15)$$

And:

$$\varepsilon_{out}^2 = \frac{1}{\sqrt{2\pi}\sigma} \left(\int_{-\infty}^{-\Delta/2} \text{err}(th^*)^2 e^{-\frac{th^{*2}}{2\sigma^2}} dth^* + \int_{\Delta/2}^{+\infty} \text{err}(th^*)^2 e^{-\frac{th^{*2}}{2\sigma^2}} dth^* \right) \quad (16)$$

For the thresholds values th^* being within the equalization range $[-\Delta/2, \Delta/2]$, the error $\text{err}(th^*)$ can be considered as a constant term, denoted by ε_d , modeling discretization error and th^* reproducibility

$$\varepsilon_{in}^2 = \varepsilon_d^2 \int_{-\Delta/2}^{-\Delta/2} \frac{1}{\sqrt{2\pi}\sigma} e^{-\frac{th^{*2}}{2\sigma^2}} dth^* \quad (17)$$

Out of the equalization range, the error is due to the difference between th^* and the best achievable correction. This best achievable correction is $-\frac{\Delta}{2}$ and $+\frac{\Delta}{2}$ in the $[-\infty, -\frac{\Delta}{2}]$ and $[\frac{\Delta}{2}, +\infty]$ ranges respectively

$$\varepsilon_{out}^2 = \frac{1}{\sqrt{2\pi}\sigma} \left(\int_{-\infty}^{-\frac{\Delta}{2}} e^{-\frac{th^{*2}}{2\sigma^2}} \left(th^* + \frac{\Delta}{2} \right)^2 dth^* + \int_{\frac{\Delta}{2}}^{+\infty} e^{-\frac{th^{*2}}{2\sigma^2}} \left(th^* - \frac{\Delta}{2} \right)^2 dth^* \right) \quad (18)$$

Developing (13) using (16) and (17) we get

$$\varepsilon^2 = \varepsilon_d^2 \text{erf}\left(\frac{\Delta}{2\sqrt{2}\sigma}\right) + \frac{\Delta^2}{4} \left(1 - \text{erf}\left(\frac{\Delta}{2\sqrt{2}\sigma}\right) \right) - \frac{2}{\sqrt{2\pi}\sigma} \Delta \exp\left(\frac{-\Delta^2}{8\sigma^2}\right) + 2 \int_{\Delta/2}^{\infty} \frac{x^2}{\sqrt{2\pi}\sigma} e^{-\frac{x^2}{2\sigma^2}} dx \quad (19)$$

Let's detail the expression of ε_d . The precision on the equalized thresholds th_{eq} due to the discretization, or threshold step, is denoted by δ and defined by

$$\delta = \frac{\Delta}{2^5 - 1} \quad (20)$$

We assume that th_{eq} has an uniform distribution in the range $[-\delta/2, \delta/2]$. The mean quadratic error due to the discretization is then, for a detector with a perfect reproductibility

$$\varepsilon_d^2 = \frac{1}{\delta} \int_{-\delta/2}^{\delta/2} th_{eq}^2 dth_{eq} = \delta^2 / 12 \quad (21)$$

To take into account the reproducibility error of th_{eq} , we assume now a Gaussian distribution of the th_{eq} values around their mean positions, which have an uniform distribution in the range $[-\delta/2, \delta/2]$. This last distribution is convolved with a Gaussian distribution with a standard deviation of σ_R , to model variations in th_{eq} between measurements

$$\varepsilon_d^2 = \frac{1}{\delta} \int_{-\delta/2}^{\delta/2} dth_{eq} \int_{-\infty}^{+\infty} \frac{1}{\sqrt{2\pi}\sigma_R} e^{-\frac{(th_{eq}-x)^2}{2\sigma_R^2}} x^2 dx \quad (22)$$

The standard deviation of the noise is assumed to be proportional to the range Δ

$$\sigma_R = \sigma_{R0} \frac{\Delta}{\Delta_0} \quad (23)$$

Finally, the development of (21) leads to

$$\varepsilon_d^2 = \frac{1}{\delta} \int_{-\infty}^{+\infty} \frac{x^2}{2} \left[\text{erf}\left(\frac{\delta/2-x}{\sqrt{2}\sigma_{R0}\frac{\Delta}{\Delta_0}}\right) + \text{erf}\left(\frac{\delta/2+x}{\sqrt{2}\sigma_{R0}\frac{\Delta}{\Delta_0}}\right) \right] dx \quad (24)$$

Acknowledgments

The authors are greatly indebted to the other members of the Medipix3 Collaboration. They would like to thank the anonymous reviewers for their valuable comments and suggestions to improve this paper.

References

- [1] P. Kraft, et al., *IEEE Transactions on Nuclear Science* NS56 (2009) 758.
- [2] P. Pangaud, et al., *Nuclear Instruments and Methods in Physics Research Section A* A591 (2008) 159.
- [3] L. Tilustos, et al., *IEEE Transactions on Nuclear Science* NS53 (1) (2006) 367.
- [4] J. Uher et al., Equalization of Medipix2 imaging detector energy thresholds using measurement of polychromatic X-ray beam attenuation, in: *Proceedings of the 13th International Workshop on Radiation Imaging Detectors*, 3–7 July, ETH Zurich, Switzerland, 2011.
- [5] E. Gimenez, et al., *IEEE Transactions on Nuclear Science* NS58 (2011) 323.
- [6] Vykydal, et al., *Nuclear Instruments and Methods in Physics Research Section A* 563 (2006) 112.
- [7] Luigi Pacciani, et al., *Nuclear Instruments and Methods in Physics Research A* 593 (2008) 367.
- [8] E. Frojdh, et al., *Journal of Instrumentation* 9 (4) (2014).